3 Neutrino Beams

3.1 General Considerations

In discussing neutrino beams and neutrino experiments one has to keep in mind two basic facts:

(a) Neutrino cross sections are very low.

(b) Neutrino beams, being tertiary in nature and not capable of being focused, tend to be large in transverse dimensions.

These two facts strongly influence the design of the neutrino experiments. We elaborate further on these points below.

The neutrino charged current cross section on a single nucleon at high energies is very roughly[18]

$$\sigma_\nu^{CC} \approx 0.7 \times 10^{-38} E_\nu\,(\mathrm{GeV})\ \mathrm{cm}^2$$

and the neutral current cross section

$$\sigma_\nu^{NC} \approx 0.3 \times 10^{-38} E_\nu\,(\mathrm{GeV})\ \mathrm{cm}^2 \ .$$

The antineutrino cross sections are smaller by roughly a factor of 2.5.

The purely leptonic processes, e.g., $\nu_e e^- \rightarrow \nu_e e^-$, have even smaller cross sections. The $\nu_e e^-$ cross section[19] is

$$\sigma^{\nu e} \approx 0.933 \times 10^{-43}\,(E_\nu / 10\mathrm{Mev})\ \mathrm{cm}^2$$

and the corresponding cross sections of $\bar{\nu}_e$, ν_μ, and $\bar{\nu}_\mu$, are about a factor of 2.4–7.1 smaller. These values have to be contrasted with a typical hadronic cross section of about 10^{-26}–10^{-25} cm^2.

As far as the beam transverse size is concerned, a typical neutrino beam in the GeV energy range will be of the order of 1 m^2 or larger. In contrast, hadron beams can be focused to spot sizes of the order of 1 mm^2 or even smaller.

Putting all of these numbers together, we see that per atom the neutrino interaction probability of a neutrino in a neutrino beam is about 18 orders of magnitude smaller than for a hadron in a hadron beam. This great disparity means that large beam intensities and massive detectors form a necessary requirement for neutrino experiments.

3.2 Beams From Accelerators

Accelerator-produced neutrino beams have played a key role in the neutrino experimental program to date. The obvious neutrino sources can be divided into three general categories, depending on the typical decay length scale of the parent particles. Examples of these three categories are enumerated in Table 1 below where the typical decay length quoted corresponds to parent energies in the multi-GeV range.

TABLE 1.
Potential sources of neutrinos from an accelerator.

<u>Long lived sources:</u> $\lambda \approx 1$ km	BR ≈ 50-100%
$\pi^+ \to \mu^+ \nu_\mu$	
$K^+ \to \mu^+ \nu_\mu,\ \ \pi^\circ \mu^+ \nu_\mu,\ \ \pi^\circ e^+ \nu_e$	
$K_L^0 \to \pi^- \mu^+ \nu_\mu,\ \ \pi^- e^+ \nu_e,\ \ \pi^+ \mu^- \bar{\nu}_\mu,\ \ \pi^+ e^- \bar{\nu}_e$	
$\mu^+ \to e^+ \bar{\nu}_\mu \nu_e$	
<u>Medium lived sources:</u> $\lambda \approx 1$ m	BR ≈ 0.1%
$\Lambda \to p e^- \bar{\nu}_e$	
$K_S^0 \to \pi^- \mu^+ \nu_\mu,\ \ \pi^- e^+ \nu_e,\ \ \pi^+ \mu^- \bar{\nu}_\mu,\ \ \pi^+ e^- \bar{\nu}_e$	
$\Sigma^- \to n e^- \bar{\nu}_e$	
<u>Short lived sources:</u> $\lambda \approx 1$ mm - 1cm	BR ≈ 2-20%
$D^+ \to K^0 \mu^+ \nu_\mu,\ \ K^0 e^+ \nu_e$	
$D_s^+ \to \tau^+ \nu_\tau$	
$\tau^+ \to \mu^+ \nu_\mu \bar{\nu}_\tau,\ \ e^+ \nu_e \bar{\nu}_\tau$	
$B^o \to D^- \mu^+ \nu_\mu,\ \ D^- e^+ \nu_e$	

It is the first category of sources that gives us the classical neutrino beams. The parent particles are relatively long lived for a variety of reasons: no lower-mass hadronic state for π, $\Delta I = 1/2$ rule for K^+, CP conservation to a high accuracy for K_L^0, and a purely leptonic process for μ^+. The last category of processes is interesting as a potential source of beam-dump neutrinos, where one wants to suppress contributions from the long lived sources.

3.2.1 Neutrinos from Hadron Beams

Even though the neutrino beams produced from hadron beams are quite diverse in their nature and the relevant beam design, the basic principle in all the cases is the same. The "generic" hadron-produced neutrino beam is shown in Fig. 3. Accelerator primary beam (generally protons) strikes a target where different hadrons are produced. Some initial focusing and momentum and/or sign selection may be done immediately downstream and hadrons are allowed subsequently to drift for some distance L. A fraction of them will decay in that space and create neutrinos collimated in a cone around the hadronic propagation direction. The drift space is terminated by a beam stop to eliminate residual hadrons; it is then followed by a shield (earth and/or iron) to absorb and stop resulting hadronic debris but also, more importantly, to range out the muons created together with the neutrinos in the hadron decays. After some distance l, generally chosen by the criterion that it has to be sufficiently long to range out even the most energetic μ's, a detector is placed where neutrino interactions are observed.

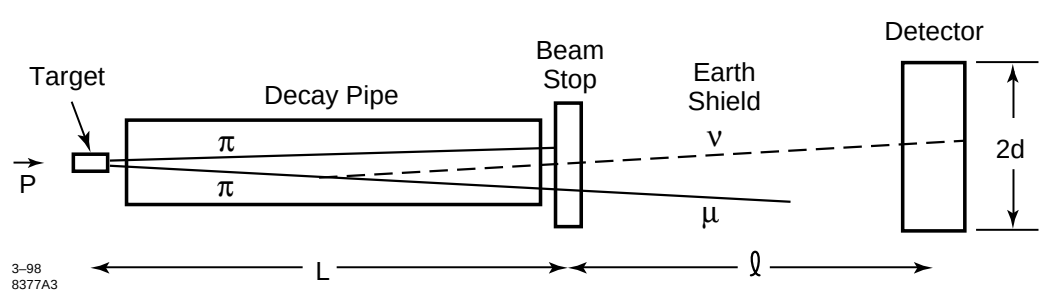

FIG. 3. Schematic of a typical accelerator neutrino beam.

To discuss the optimization of neutrino beams, we need to review first some basic kinematics. We recall that

$$E_\nu^{lab} = \gamma\,(\beta P_\nu^{*} \cos\theta_\nu^{*} + E_\nu^{*}),$$

where the starred quantities refer to π or K rest frame. Because $m_\pi \sim m_\mu$, but $m_K >> m_\mu$ we have

$$E_\nu^{lab,\ max} \approx 0.41\ \ P_\pi^{lab} \quad \text{(for } \pi \text{ decay)},$$

$$E_\nu^{lab,\ max} \approx P_K^{lab} \quad \text{(for } K \to \mu\nu \text{ decay)}.$$

The median laboratory angle, corresponding to $\theta_\nu^{*} = \pi/2$ will be given by $\theta^{med} = 1/\gamma$.

We can now ask what should be the values of L, l, and 2d (transverse size of the detector) required so that the detector can intercept a significant fraction of <u>potentially</u> produced ν's. Such a condition might be defined as one corresponding to L of the order of hadronic lifetime ($\approx \gamma c \tau_{had}$) and the detector size sufficient to intercept more than half of the neutrino flux. The requirement that even the most energetic μ's are absorbed means that for the earth shield

$$l\ (\text{km}) \approx 2P_{had}\ (\text{GeV}),$$

since μ's lose roughly 0.5 GeV/m of earth shield. We have then $L \approx \gamma c \tau$ and $d \propto (L + l)\,\theta^{med} = \frac{1}{\gamma}(L + l)$. We see that for such a design d is independent of the primary hadron energy, since both L and l scale as this energy.

For 50 GeV π's, we would have

$$\gamma \approx 350,$$

$$L \approx 2.7 \text{ km},$$

$$l \approx 100 \text{ m, and}$$

$$d \approx 8 \text{ m}.$$

Clearly, such a detector is uncomfortably large and drift space uncomfortably long. Obviously, the above parameters need to be scaled down and we need to consider how to optimize the overall design.

To zeroth order, the number of observed ν interactions near 0° scales as d^2z, z being the depth of the detector. The cost, also to zeroth order (i.e., ignoring initial fixed costs and economies of scale), scales similarly as d^2z. To go beyond zeroth order analysis, we must consider factors which break this degeneracy, i.e.,

(a) ν spectrum is not flat but falls off as we go away from 0° (towards larger d).

(b) E_ν variation with θ near 0° is

$$E_\nu = \frac{E_\nu^{max}}{1 + (\gamma\theta)^2} \quad .$$

Thus E_ν, and hence σ_ν, falls off as θ increases.

Both of these factors argue for largest possible z (i.e., small d). However, we have to consider the need to define a fiducial volume; this requirement establishes some minimum transverse dimension of the detector, d. Thus the dimensions of the detector need to be optimized in light of these three conditions and the precise cost dependence.

To optimize L for maximum flux, we need to find an optimum compromise between the decreasing hadron flux as one goes away from the target production due to exponential decay of the hadrons and an increasing acceptance as the decays occur closer to the detector, and hence further away from the production target. We generally try to make l as small as possible, consistent with adequate shielding. The conditions chosen in the past for a typical experiment were

$$l < L < 2l$$

and d of the order of 1–2 m. We emphasize that such values are appropriate for optimization which tries to maximize the number of detected neutrino events.

We can turn now to the discussion of specific hadron-beam originated neutrino beams. The simplest such beam is a “bare target” beam which was used in the first neutrino accelerator experiment.[4] No focusing of the hadrons is attempted in this situation and hence, the neutrino yield at the detector is rather low. Since that first experiment, many different schemes have been developed to obtain enhanced neutrino yields or beams with specific neutrino properties.

Clearly, the neutrinos themselves cannot be focused. Thus, we always have to live with the neutrino divergence due to the intrinsic P_T in the decay: 30 MeV/c for $\pi \to \mu\nu$ decay, 236 MeV/c for $K^+ \to \mu^+\nu$ decay. However, in a bare target beam, there is also the additional divergence of the hadronic beam, characterized by a typical P_T in the production process of about 300 MeV/c. This component could be eliminated or drastically reduced by the appropriate focusing. In an ideal case, never achieved in practice, the hadrons would form a perfectly parallel pencil beam in the drift space.

One of the earliest schemes[20] used to obtain hadron focusing (still in use today) relies on pulsing a current through an appropriate conducting surface, shaped so as to generate a focusing magnetic field. Several such elements, referred to as "horns," can be combined to obtain focusing over a broad momentum range. One such geometry, proposed for the MINOS experiment to be discussed later, is illustrated in Fig. 4. The current flows on the inside surface and returns on the outside surface. From Ampere's law we have

$$\text{inside the cone: } B = 0,$$
$$\text{in the horn: } B \propto 1/r, \text{ and}$$
$$\text{outside horn: } B = 0.$$

For the parallel track, the path length inside the horn (in the finite B region) is proportional to r. Thus, the total transverse momentum kick given to each particle will be

$$P_T \propto \int B \cdot dl \propto \frac{1}{r} \cdot r = \text{constant (independent of r).}$$

Thus, the horn will be focusing particles of one sign and defocusing the particles of the opposite sign, provided that they go through the horn. Trajectories inside or outside the horn will be unaffected. Focusing will be perfect for particles of a given P_T.

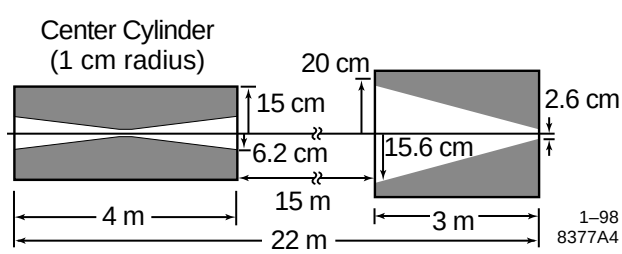

FIG. 4. Current design of the focusing horn system to be used in the NuMI beam for the COSMOS and MINOS experiments.

In practice, to focus a spectrum of particles with various values of P and P_T, more complicated systems are designed. One can vary in such a design a number of parameters, i.e.:

number of horns used,

separation between individual horns,

dimensions and shape of the horns, and

field strength (i.e., current).

A properly designed horn system can enhance neutrino flux significantly: gains of more than a factor of ten are possible. This is illustrated in Fig. 5 where we show neutrino yields for a double horn system and an unfocused system for a potential ν beam at Brookhaven National Laboratory.[21] Typical horn designs today can achieve, in the selected momentum range, neutrino collection efficiencies of the order of 50% of what one could obtain with a perfectly focused beam, i.e., one that is exactly parallel. This is illustrated in Fig. 6 where the MINOS horn design[22] is used to demonstrate this ratio as a function of momentum. The focusing efficiency as a function of neutrino energy can be changed by varying the horn parameters.

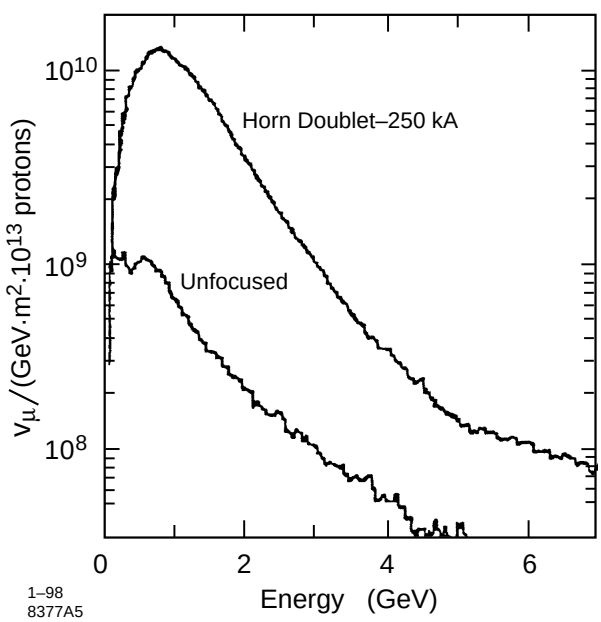

FIG. 5. Relative fluxes for an unfocused and double-horn focused beams for a BNL neutrino beam design.

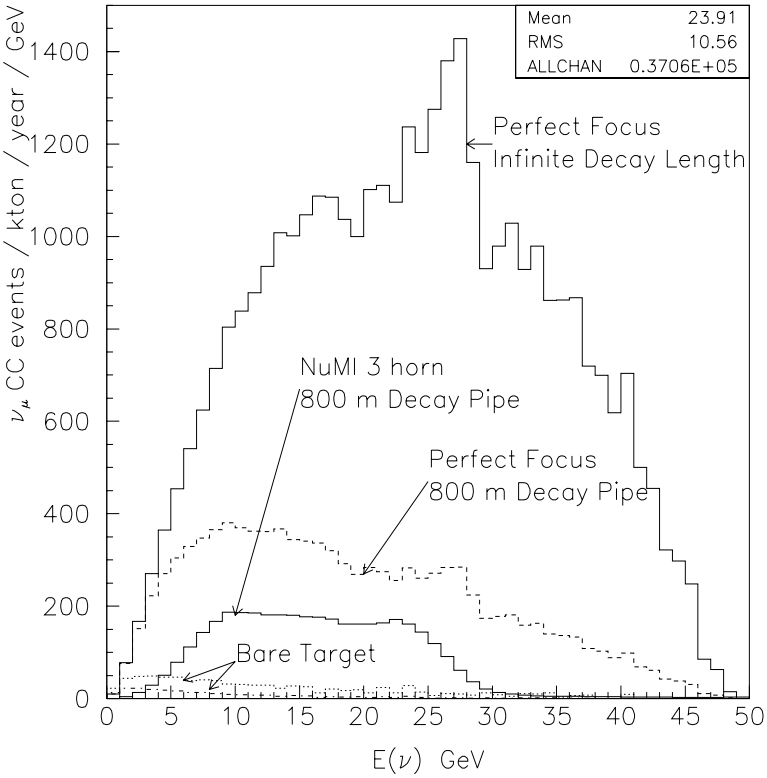

FIG. 6. Focusing efficiency as a function of neutrino energy for the NuMI horn design compared to fluxes obtained in ideal conditions and fluxes from a bare target.

Other focusing arrangements are also possible and a number of them have been used in actual experiments. The most important ones are:

(a) Quadrupole focused beam—both signs of hadrons are focused and the magnet settings are chosen to pick out a desired broad momentum range. The neutrino momentum spectrum for such a beam for the CCFR experiment at Fermilab[23] is shown in Fig. 7.

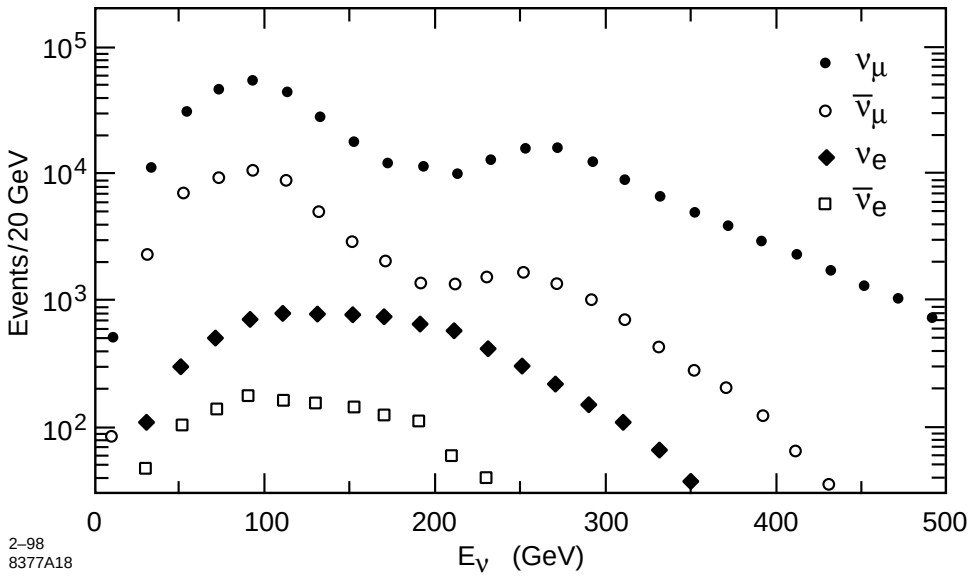

FIG. 7. Neutrino event rates from the four different neutrino flavors in the CCFR detector exposed to the Fermilab quadrupole focused beam. The ν_e (and $\bar{\nu}_e$) rates have been calculated by Monte Carlo with the normalization for the measured rates of the ν_μ and $\bar{\nu}_\mu$ flavors.

(b) Sign-selected quadrupole focused beam—this is a variant on the previous possibility with an addition of an upstream dipole magnet to select only one sign of hadrons, and hence only neutrinos or antineutrinos at the detector. The recently completed E815 experiment at Fermilab used this configuration.

(c) Dichromatic beam—such a beam uses dipoles and quadrupoles to define a relatively narrow accepted momentum band of the hadrons. The neutrino energies from π and K two-body decays are given by

$$E_\nu^\pi = \frac{m_\pi^2 - m_\mu^2}{2\,(E_\pi - P_\pi \cos\theta)}, \qquad E_\nu^K = \frac{m_K^2 - m_\mu^2}{2\,(E_K - P_K \cos\theta)},$$

$\cos\theta$ being the laboratory angle of the neutrino with respect to the beam axis. Because $m_K \approx 3.5\, m_\pi$, the neutrinos emitted at 0°, which come from K decays, will have a significantly higher energy than those from π decays. Furthermore, if the detector subtends an angle that is small compared to the total neutrino emission cone, the two spectra will be relatively monochromatic, hence the name dichromatic beam. This is illustrated in Fig. 8 where we show the neutrino energy spectra for the first dichromatic beam constructed at Fermilab.[24]

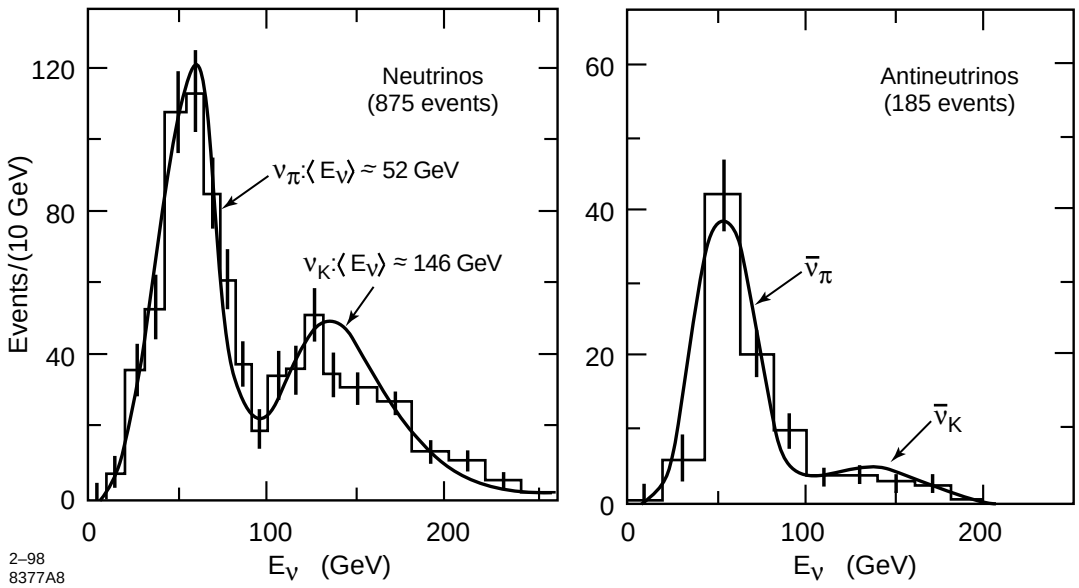

FIG. 8. ν_μ and $\bar{\nu}_\mu$ spectra (expressed in terms of observed events) for the first dichromatic beam constructed at Fermilab.

Generally, the detector subtends a significant fraction of the neutrino emission cone. In such a situation, a large part of the neutrino spectrum will be sampled, with a direct correlation between the emission angle (i.e., roughly the distance of the interaction from the beam axis in the detector) and the neutrino energy, as can be seen from the equations above. Clearly, this correlation is different for ν's with π parentage from these originating from K decays.

In principle, at least, such a correlation can be exploited to get a “good fix” on the neutrino energy. Such a situation was true in the CDHS experiment at CERN,[25] but to my knowledge this energy-angle correlation was never exploited in any physics analysis.

In addition to the focusing systems described above, other variants of neutrino beams have been proposed but never executed to my knowledge. The two important ones are:

(a) Tagged ν beams. The idea here is that by detecting the charged decay product(s) from hadron decay in coincidence with the ν event, one can obtain information about the energy and/or flavor of the neutrino causing the interaction. To date, no tagged ν beams have been implemented, even though a number of different possibilities have been discussed. The main problem in executing such a scheme

is the high counting rate in the potential detector exposed to the charged decay products. Some of the possibilities that have been discussed are:

(i) Measure momentum and angle of the μ^+ in $K^+ \to \mu^+\nu$ decay. Thus, one can obtain the energy of the neutrino.

(ii) Detect μ or e in the $K_L^0 \to \pi e(\mu)\nu$. This will allow one to determine the neutrino flavor.

(iii) Detect the e^+ in $K^+ \to \pi^0 e^+\nu$. This would allow one to veto such decays and thus obtain a purer sample of ν_μ's. The $K^+ \to \pi^0 e^+\nu$ decay is one of the main factors limiting the sensitivity of $\nu_\mu \to \nu_e$ oscillation searches because of the ν_e contamination from this decay occurring at about a 0.5% level.[26]

(b) Off-axis beam. This idea basically allows you to obtain a relatively monochromatic low energy beam at the expense of flux.[27] The basic principle of such a beam is illustrated in Fig. 9. As can be seen, at non-zero angles, a large energy band of π's generates a rather monochromatic neutrino beam.

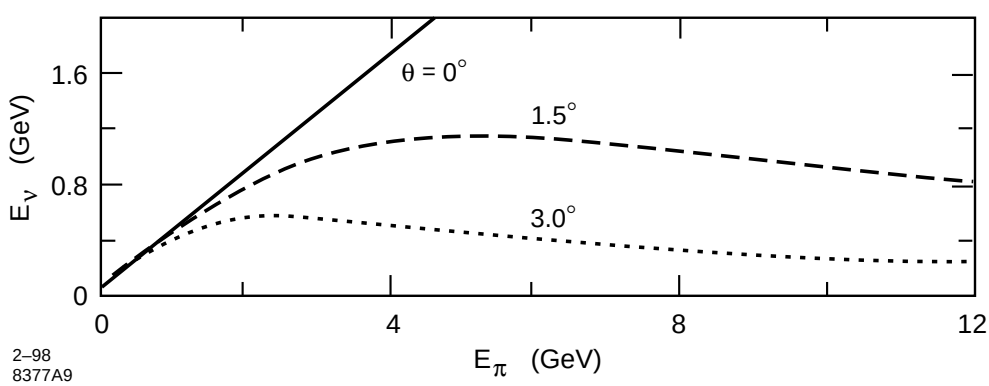

FIG. 9: Neutrino energy as a function of the parent π energy and of the laboratory decay angle.

3.2.2 Neutrinos from Beam Dumps

This method of producing neutrino "beams" differs from the one discussed above in so far that no secondary hadron beam is ever produced. We define the beam dump as a source of ν's as that experimental configuration in which the target for the primary (e.g., most likely proton) beam, in which the ν parent hadrons are produced, is at the

same time also the medium for absorbing and/or stopping these hadrons. Thus, no drift space is provided for the hadrons to decay in.

The beam-dump neutrino experiments naturally divide themselves into two categories: high energy and low energy ones. We discuss each one in turn.

(a) The general motivation for high energy beam-dump experiments is to eliminate or drastically reduce the contributions of ν's from long lived and medium lived sources, described as categories 1 and 2 in Table 1. In this configuration, one could look for neutrinos from the third category of sources. i.e., decays of short lived particles, or for some new and unanticipated phenomenon.

Historically, the first beam dump experiment of this type was proposed and executed in the late '60's by Mel Schwartz and his collaborators at SLAC,[28] using the 20 GeV SLAC electron beam and optical spark chambers downstream. This was before the first observation of neutral currents and before the discovery of charm, beauty, and τ. Because of financial considerations, the design of the experiment had to be somewhat compromised and the detector moved further away from the beam dump than initially desired. The decrease in sensitivity due to this compromise contributed to a null result.

One of the first observations of charm production in hadronic interactions came from a CERN beam-dump experimental program[29] which used several detectors downstream to detect neutrinos, produced by the decays of charm particles, which in turn were produced by interactions of the primary proton beam in the dump.

The present interest in high energy beam-dump experiments is driven by the desire to observe ν_τ, a neutrino flavor known to exist from indirect evidence but never to date observed experimentally. The experiment E872 at Fermilab,[30] currently in progress, has been designed to look for ν_τ's from the production and decay of D_s mesons, the decay chain of interest being

$$D_s \rightarrow \tau + \nu_\tau \text{ and/or } \tau \rightarrow X + \nu_\tau$$

where X is some hadronic or leptonic system. The experimental challenge in the beam design is to minimize the beam-dump to detector distance and thus maximize the ν_τ event rate and at the same time keep the backgrounds in the detector from the dump down to a manageable level. The beam used for the E872 experiment is illustrated in Fig. 10. With this design, about 4% of all ν's in the detector should be ν_τ's.

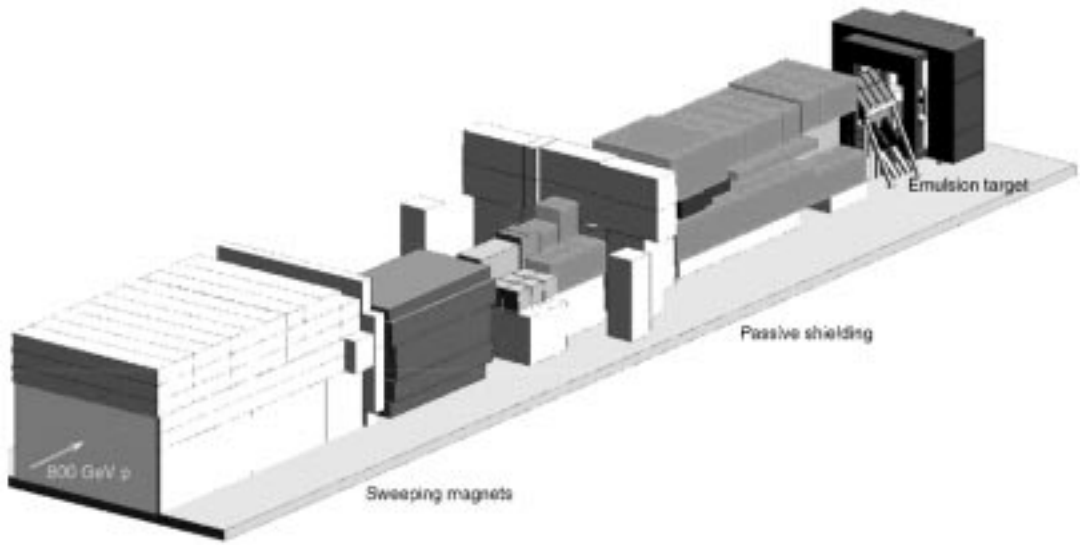

FIG. 10. E872 beam-dump beam.

(b) The low energy beam-dump experiments are designed to look at interactions of neutrinos from decays of μ^+ and π^+ stopped in the dump. This way, one can obtain a well-understood, in terms of energy and flavor, neutrino flux radiating isotropically out from a relatively small volume. If the proton beam is extracted in short bunches, one can use the time of arrival of neutrinos to determine their flavor and energy. This point is elaborated in Fig. 11. Figure 11(a) shows the neutrino energy spectra resulting from π^+ and μ^+ decay at rest. Because the lifetime of π^+ is significantly shorter than that of μ^+, the monochromatic ν_μ's from π^+ decay occur shortly after the proton beam pulse (within tens of nanoseconds); the ν_e and $\bar{\nu}_\mu$'s from μ^+ decay are spread out over a much longer period of time, i.e., of the order of microseconds due to the 2.2 μsec μ^+ lifetime. The time structure of the ν's from the ISIS spallation source at the Rutherford Appleton Laboratory[31] accelerator is illustrated in Fig. 11(b) and 11(c). In that machine, protons are extracted at a 50 Hz rate with each major pulse consisting of two short pulses about 300 nsec apart.

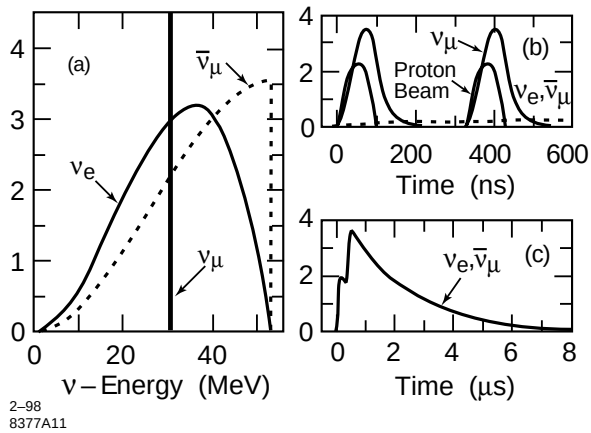

FIG. 11. The principle of a low energy beam-dump experiment. The neutrino spectra from π at rest (ν_μ) and μ at rest (ν_e and $\bar{\nu}_\mu$) are shown in (a). The time structure of the different flavor neutrinos is shown in (b) and (c) for the ISIS machine.

3.2.3 Other Accelerator-Produced Beams

There are other potential ways to use accelerators to produce neutrino fluxes for experiments. The two that have been discussed the most extensively are ν's from interaction regions and ν's from storage rings. The first method relies on the fact that high energy pp colliders, like the LHC, will produce charm and beauty particles copiously. They will generally tend to be produced in a forward direction and will decay promptly. The neutrinos from these decays will also be collimated forward reasonably well. Because π's and K's will tend to be absorbed in the calorimeters forming part of the detector, the neutrino "beam" will be dominated by products of charm decays and will have roughly equal components of ν_μ, $\bar{\nu}_\mu$, ν_e, and $\bar{\nu}_e$. In addition, one expects about 10% of the ν flux to be ν_τ's, mainly from D_s decays but with some contribution from B decays. Detailed calculations of potential ν fluxes at the LHC have been made, first by De Rújula[32] and more recently by Fernández.[33]

Another potentially interesting source of neutrinos is a storage ring for unstable particles, e.g., π's, K's or μ's. If a significant fraction of the storage ring circumference is a straight section, the decays in that section will produce a well-collimated ν beam. Interest in such a possible ν source has been recently revived[34] in connection with the studies of a possible $\mu^+\mu^-$ collider in the TeV range. The μ intensity required to obtain sufficiently high collision luminosity (typical numbers discussed are few x 10^{12} μ's/bunch at 15 Hz) is so high that the ν fluxes from such a

source would be more copious than any hitherto available. Neutrino interaction rates in a typical ν detector might be of the order of few KHz.

3.3 Neutrinos from Reactors

Nuclear fission, which is the energy mechanism in a reactor, yields neutron-rich nuclear fragments as by-products. These will be unstable and decay by the fundamental process

$$n \text{ (in nucleus)} \rightarrow p\ e^-\ \bar{\nu}_e\,.$$

The ν flux is related directly to thermal power and is roughly $2 \times 10^{20} \bar{\nu}_e$/GW/sec. Clearly the neutrinos are emitted isotropically.

The ν spectra obtained from reactors are now quite well understood at the level of about 2—3%. The calculations have been verified experimentally.[35] At the low end of the spectrum there is an additional correction that needs to be made to allow for decays of the activated material in and near the core. A typical positron spectrum from reactor neutrino interactions is shown in Fig. 12. The neutrino energy is 1.804 MeV higher than the positron energy.

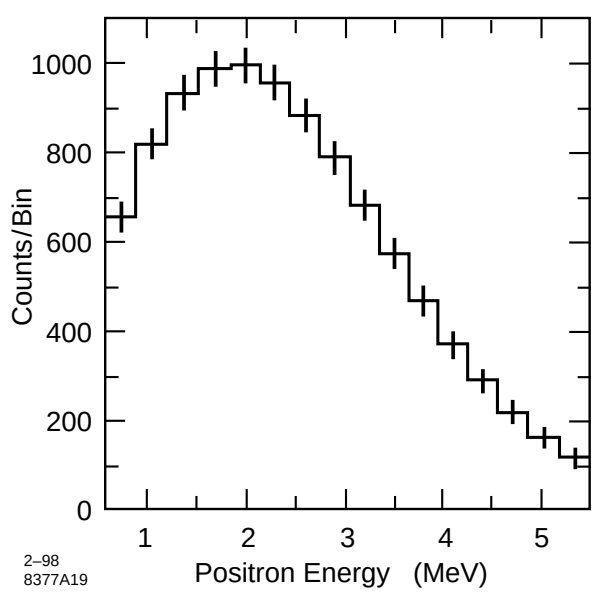

FIG. 12. Positron spectrum expected from neutrino interactions in the CHOOZ experiment (assuming no oscillations).

In addition, reactors have been used to create man-made neutrino sources by activating materials. This technique has been used to create sources whose decay neutrinos were subsequently used to calibrate solar neutrino detectors, e.g., GALLEX

and SAGE.[36] In this scheme ^{50}Cr is irradiated with neutrons from a reactor to give ^{51}Cr which is unstable and gives ν's in the energy range comparable to the one characterizing the solar neutrino spectrum. Sources of 100 BCq have been obtained via this method. Figure 13 shows data from one of the GALLEX calibration runs using such a source. As required for such a calibration, neutrino flux from the source is significantly higher than the solar flux.

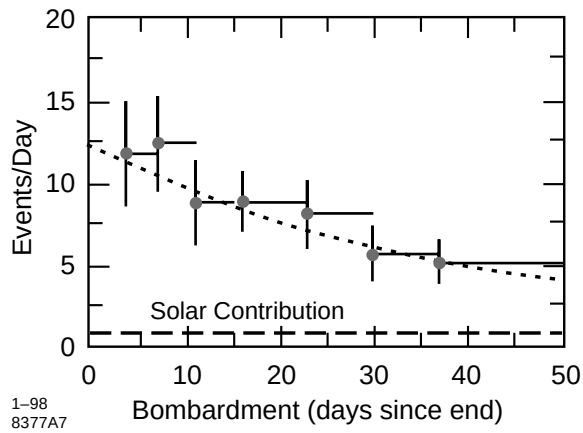

FIG. 13. The observed counting rate from the GALLEX experiment during the chromium source calibration runs. The points for each run are plotted at the beginning of each exposure; horizontal lines show duration of the exposure. The dotted line shows the predicted behavior, calculated from the directly measured source strength and the known half-life of ^{51}Cr.

3.4 Neutrinos from Natural Sources

For completeness I shall close this chapter by saying a few words about neutrinos from naturally occurring sources.

(a) Neutrinos from the sun. The sun is essentially a fusion reactor, effectively transforming four protons into a He^4 nucleus through a fusion process that reduces to

$$4p \rightarrow He^4 + 2e^+ + 2\nu_e.$$

Thus, the number of neutrinos emitted can be readily obtained from the total thermal power of the sun which is in turn directly related to the measurable quantity, i.e., the solar constant, 1.3 kW/m^2 on the surface of the earth. The spectrum of the neutrinos emitted will depend on the details of the energy producing solar cycle. Precise knowledge of this spectrum is important in the

interpretation of the experimental data on solar neutrino interactions on earth. The spectrum prescribed by the current Standard Solar Model[37] is shown in Fig. 14.

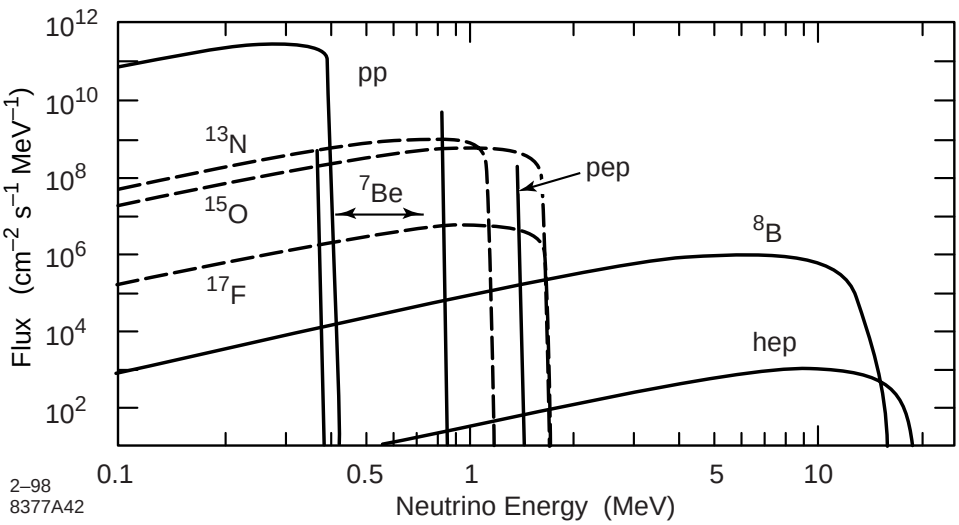

FIG. 14. Energy spectra of solar neutrinos. The pp chain is indicated by the solid curves; the less important CNO cycle by dashed curves.

It is amusing to compare the two power sources that both generate neutrinos, i.e., the sun and reactors. Such a comparison of the relevant quantities is made in Table 2.

TABLE 2.

Comparison of sun and reactor as ν sources.

Feature	Sun	Reactor
Process	Fusion	Fission
yield	1.8 x 10^{38} ν/sec	2 x 10^{20}ν/GW/sec
ν Flavor	ν_e	$\bar{\nu}_e$
Energy Spectrum	Peaks sharply below 1 MeV Extends up to 15 MeV	Few MeV
Understanding of spectrum	Some controversy	Very good
Possibility to vary L	Very little (yearly variation)	Yes
On/off capability	No	Yes

(b) Atmospheric neutrinos. The energetic hadronic particles constantly bombarding our atmosphere will generally interact in the first 10% or so of the atmosphere by weight, i.e., at about 10-20 km above the earth's surface. The density of air at that altitude is such that most of the π's and K's in the GeV range and below which are produced there will decay before interacting and most of the resulting daughter μ's will also decay. These decays (as well as the decays of subsequent generations of hadrons) are the source of the so called atmospheric neutrinos. The spectrum of these neutrinos peaks at low energies (few hundreds MeV's) and falls off as we go to the multi-GeV range. Because the relevant ν production processes are

$$\pi^+ \to \mu^+ \nu_\mu,$$
$$\mu^+ \to e^+ \nu_e \bar{\nu}_\mu,$$

the ratio of muon to electron neutrinos at low energies, where most of the μ's decay, should be about two. This ratio will increase as we go to higher energies.[38] The particles produced at different zenith angles will see different variations in atmospheric density as a function of their path. This, plus the effect of the earth's magnetic field, generates a different zenith dependence of the ν_μ and ν_e fluxes which is energy dependent.

(c) Neutrinos from supernovae. Neutrinos are generated in a supernova explosion[39]both from the inverse beta decay process, i.e.,

$$p + e^- \to n + \nu_e$$

and also through e^+e^- annihilation, i.e.,

$$e^+ + e^- \to \nu + \bar{\nu}.$$

The latter process can give neutrinos of all three flavors. Supernova neutrinos have energy in the range of MeV to tens of MeV. Their theoretically expected features have been roughly verified experimentally in the observation of ν's from the supernova SN1987A.[40]

(d) Neutrinos from extragalactic sources. Neutrinos can potentially be produced copiously in various "exotic" stellar phenomena and they might have very high energies.[41] Such possibilities imply that neutrinos might open up a new window for study of the universe since they can travel a long way and are not affected by electromagnetic fields. Observation of these neutrinos is one of the motivations

for construction of large, high energy neutrino-detecting arrays like AMANDA,[42] NESTOR,[43] etc.

(e) Neutrinos from natural radioactivity. Our universe contains a number of naturally occurring neutrino emitters. Studies of such radioactive nuclei played an important role in the development of the V-A theory of weak interactions even though such neutrinos themselves have never been detected (to my knowledge). The neutrinos from the naturally occurring radioactivity in the earth's core might actually be a relevant background for some of the new ambitious reactor neutrino experiments[44] being planned currently.

In Fig. 15, we try to compile and summarize in one place in a more quantitative way the information discussed in this chapter. The figure is meant to give only a rough indication of the ν energies and fluxes from the most important sources.

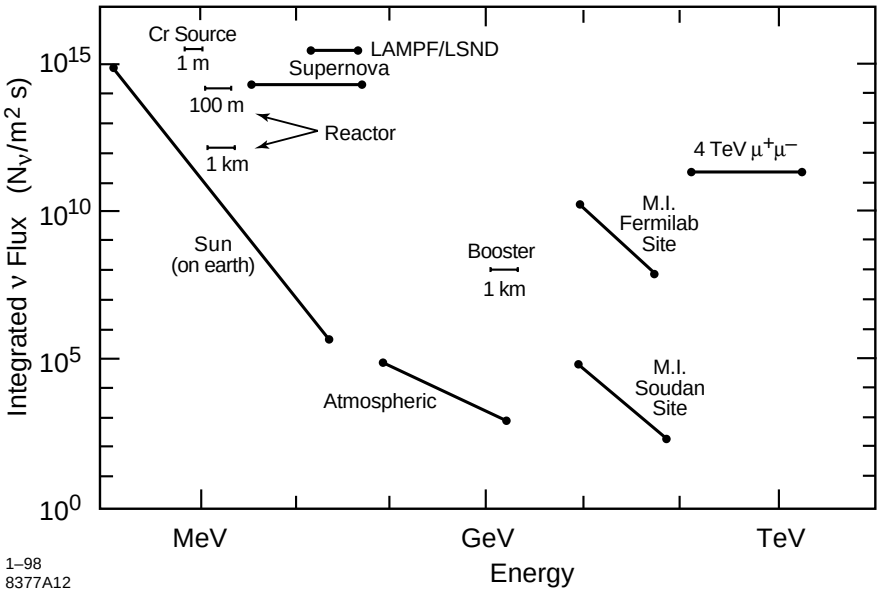

FIG. 15. A rough estimate of the neutrino fluxes from different possible sources. Booster and M.I. refer to the Booster and Main Injector rings at Fermilab; LAMPF/LSND to an accelerator/detector at Los Alamos.